Pis'ma v ZhETF, vol. 76, iss. 7, pp. 483 – 487 © 2002 October 10

Search for the neutrino radiative decay with the prototype of the Borexino detector

A. V. Derbin[1)], *O. Ju. Smirnov*[+1)]

St.Petersburg Nuclear Physics Institute RAS, 188350 Gatchina, Russia

[+]*Joint Institute for Nuclear Research, 141980 Dubna, Russia*

Submitted 16 July 2002

Resubmitted 22 August 2002

Results of background measurements with the prototype of the Borexino detector have been used to obtain bounds on the lifetime of the radiative neutrino decay $\nu_H \to \nu_L + \gamma$. The new lower limit for the lifetime of *pp* and ^{7}Be neutrinos is $\tau_{c.m.}(\nu_H \to \nu_L + \gamma)/m_\nu \geq 4.2 \cdot 10^3\,\mathrm{s} \cdot \mathrm{eV}^{-1}$ ($\alpha = 0$). It is more than one order of magnitude stronger than obtained in previous experiments using nuclear reactors and accelerators.

PACS: 13.15.+g, 14.60.Pq

1. If neutrinos have mass, then the heavier one can decay to the lighter one $\nu_H \to \nu_L + \gamma$. In the Standard model (SM) the life time of the neutrino expressed in terms of the transition magnetic moment μ^{tr}_{HL} is [1 – 4]:

$$\tau[s] \approx 0.19 \left(\frac{\mu_B}{\mu^{tr}_{HL}}\right)^2 \left(\frac{m^2_{\nu_H}}{m^2_{\nu_H} - m^2_{\nu_L}}\right) \left(\frac{1eV}{m_{\nu_H}}\right)^3 \qquad (1)$$

where μ^{tr}_{HL} is in Bohr magneton (μ_B) units. The probability of radiative decay in SM is very low. If the neutrino transition moment μ^{tr}_{HL} has a value close to that expected for a diagonal magnetic moment $\mu_\nu \approx 3.2 \cdot 10^{-19}(m_\nu/1\mathrm{eV})\mu_B$, then from (1) the lifetime of the neutrino is $\tau \sim 10^{29}$years. At the same time, the reasons (the same as for the right boson) that lead to a large magnetic moment also lead to an increase of the probability of radiative neutrino decay [5 – 9].

The radiative decay of the reactor antineutrinos $\overline{\nu_e}$ have been studied in [10 – 14]; the latter gives the best lifetime lower limit of $\tau_{c.m.}/m_\nu \geq 200\ \mathrm{s} \cdot \mathrm{eV}^{-1}$ (90% c.l.). The search for the ν_μ and $\overline{\nu_\mu}$ decays was performed in a high intensity beam of neutrinos from π^+ and μ^+ decaying at rest; the lifetime of the muon (anti)neutrino was bounded $\tau_{c.m.}/m_{\nu_\mu} \geq 15.4\,\mathrm{s} \cdot \mathrm{eV}^{-1}$ [15]. A much more restrictive limit was obtained from the solar γ-ray flux, $\tau_{c.m.}/m_{\nu_e} \geq 7 \cdot 10^9\,\mathrm{s} \cdot \mathrm{eV}^{-1}$ [16]. The astrophysical limits are even more stronger, and lie in the region $10^9 - 10^{20}$ s/eV [17 – 19] and references therein).

In this paper we present the results of the search for the neutrino radiative decay with the prototype of the Borexino detector.

2. Experimental set-up and results of measurements. Borexino, a real-time detector for low energy neutrino spectroscopy, is near completion in the underground laboratory at Gran Sasso (see recent [20] and references therein). The main goal of the detector is the direct measurement of the flux of ^{7}Be solar neutrinos of all flavours via neutrino-electron scattering in an ultra-pure liquid scintillator.

The prototype of the Borexino detector – Counting Test Facility (CTF) – was constructed with the aim to test the key concept of Borexino, namely the possibility to purify a large mass of liquid scintillator at the level of contamination for U and Th of a few units 10^{-16} g/g. As a simplified scaled version of the Borexino detector, a volume of liquid scintillator is contained in a 2 m diameter transparent inner nylon vessel mounted at the center of an open structure that supports 100 phototubes (PMT) [21]. The whole system is placed within a cylindrical tank (11 m in diameter and 10 m height) that contains 1000 tons of ultra-pure water, which provides a 4.5 m shielding against neutrons originating from the rock, and against external γ-rays from PMT's and other construction materials. Detailed reports on the CTF have been published [20 – 25].

The energy of an event in the CTF detector is defined using the total collected charge from all PMTs. The coefficient linking the event energy and the total collected charge is called light yield (or photoelectron yield). The light yield for the electrons can be considered linear with respect to its energy, only for energies above 1 MeV. At lower energies the phenomenon of "ionization quenching" violates the linear dependence of the light yield on energy [26]. The deviations from the linear law can be taken into account by the ionization deficit

[1)] e-mail: derbin@lngs.infn.it; smirnov@lngs.infn.it

function $f(k_B, E)$, where k_B depends on the scintillator properties. The total collected charge in this case is $Q \sim Ef(k_B, E)$.

Because of the non-linear dependence of the light yield on the energy released due to the ionization quenching effect, the CTF resolution should be expressed in terms of the total registered charge, which is directly measured in the experiment.

The study with the radioactive sources placed at the different positions inside the CTF inner vessel showed that the CTF response can be approximated by a Gaussian, with sigma defined by the following formula:

$$\sigma_Q = \sqrt{(1+\overline{v_1})Q + v_p Q^2}, \qquad (2)$$

where $Q = A \cdot E \cdot f(k_B, E) \cdot v_f$ is the mean total registered charge for the events of energy E distributed over the detector's volume; v_1 is the relative variance of the PMT single photoelectron charge spectrum ($\overline{v_1}$=0.34); A is the scintillator specific light yield measured in photoelectrons per MeV (A = 350 p.e./MeV in CTF-II for the event at the detector's center); v_f is the volume factor, coming from the averaging of the signals over the CTF volume. The parameters v_p=0.0023 and v_f=1.005 give additional signal variance for the source distributed over the detector's volume in comparison to the point-like source at the detector's center. The last case will naturally yield $v_p = 0$ and $v_f = 1$. All the parameters in (2) were defined with satisfactory precision from the CTF-II data (see [27, 28] for the details). For estimates of the energy resolution one can use the approximation $\sigma_E/E \approx \sigma_Q/Q$.

The experimental spectra of the CTF-II set-up in the energy region up to 450 KeV accumulated during 32.1 days of measurements are shown in fig.1. The spectrum without any cuts is shown on the top. The next distribution is obtained with the muon veto, which suppressed the background rate only 25% in this energy region. Time-correlated events (occurring in the time window $\Delta t \leq 8$ ms) and events with reconstructed radius $r \geq$100 cm (i.e. outside of the inner vessel) were also removed. Additional α/β discrimination was applied to eliminate contribution from α particles. The remaining background rate at 300 KeV of 0.05 counts/KeV·kg·yr is the lowest value achieved at any large-scale low-background installation.

The major part of the remaining background in the energy region up to 200 KeV is induced by β-activity of ^{14}C. Another source of background is the soft part of the spectra of β and γ coming from the decay of ^{40}K present in construction materials (decays occur out of the scintillator volume).

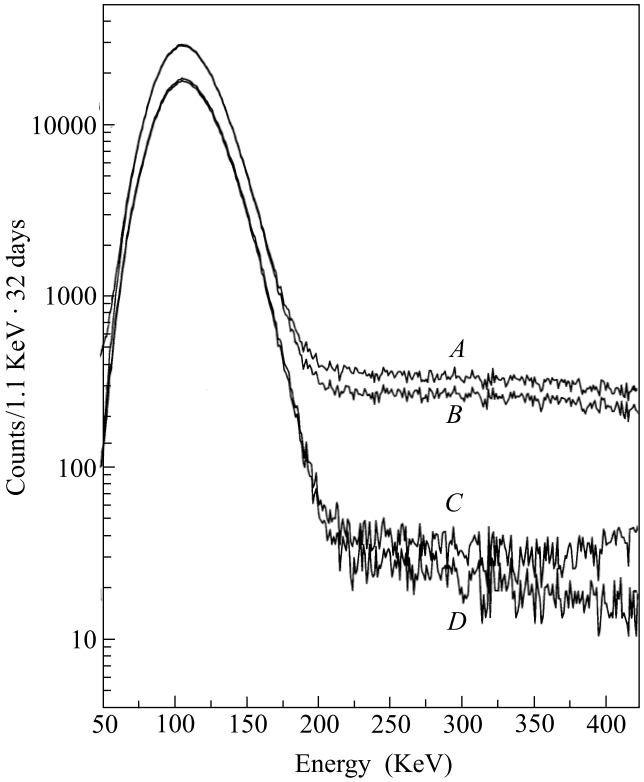

Fig.1. CTF-II background in the low energy region, and the result of the sequential cuts applied in order to reduce the background: A) raw data; B) muons cut; C) radial cut (with 100 cm radius); D)α/β discrimination

The β-decay of ^{14}C is an allowed ground-state to ground-state ($0^+ \to 1^+$) Gamow-Teller transition with an endpoint energy of E_0 = 156 KeV, and half life of 5730 years. Deviations from the allowed shape of the ^{14}C spectrum are usually parametrized as $C(E) = 1 + \alpha E$. Although the β-decay of ^{14}C was investigated by many groups over almost 50 years, the situation with the shape factor is still nuclear [29]; we leave this parameter free in our estimations.

The model function for the remaining background was selected as the sum of the ^{14}C spectrum and a first order polynomial for the underlying background:

$$S^{\mathrm{Model}}(Q) = N_0 S^{\beta}(Q, \{A, k_B, \alpha\}) + a + b \cdot Q, \qquad (3)$$

with 6 free parameters: N_0 is the number of ^{14}C decays; A is the scintillator light yield; k_B is the quenching factor; α is the ^{14}C shape factor; a, b are the parameters describing the linear underlying part of the residual spectrum.

The end-point energy of the ^{14}C spectrum was defined in other experiments with high accuracy E_0 = = (156 ± 0.5) KeV, and is fixed in the calculations.

Anyway, this parameter is in strong correlation with the parameter A, and its uncertainty is masked by the uncertainty in the parameter A. The maximum likelihood method was used to find the best values of the free parameters of the model function. The good agreement of the proposed model with the experimental data in the energy region 138–380 KeV was obtained(χ^2=205/214).

3. Analysis. The analysis is performed with the assumptions that the decaying neutrino ν_H is dominantly coupled to the electron ($U_{eH} \approx 1$) and in the final state ν_L the neutrino mass is vanishing (i.e. $m_{\nu_L} \ll m_{\nu_H}$). The expected laboratory gamma spectrum is defined by a photon moment distribution in the center-of-mass system. For the common case one can write the photon angular distribution in the general form [11]:

$$dN = \frac{1}{2}(1 + \alpha \cos(\theta))d\cos(\theta). \qquad (4)$$

The anisotropy parameter α defines the angular distribution of the photon relative to the spin of the decaying neutrino in the neutrino rest frame, and is related to the space-time structure of the decay vertex. For the Majorana neutrino, α is identically zero ($\alpha = 0$), but can take on any value $-1 \leq \alpha \leq 1$ for the Dirac neutrino. With the assumption of total parity violation, the generated left (right) – handed Dirac neutrinos correspond to the case $\alpha = -1(+1)$. The lab-frame energy of the decay gamma E_γ in the terms of the lab-frame energy of the neutrino E_ν, and the center-of-mass angle θ is:

$$E_\gamma = \frac{E_\nu}{2}(1 + \frac{P_\nu}{E_\nu}\cos(\theta)). \qquad (5)$$

After the relativistic time dilation one obtains the gamma energy spectrum E_γ due to the decay of the neutrino with energy E_ν:

$$\frac{dN}{dE_\gamma}(E_\gamma, E_\nu) = \frac{m_\nu}{\tau_{c.m.}}\frac{1}{E_\nu^2}(1 - \alpha + 2\alpha\frac{E_\gamma}{E_\nu}), \qquad (6)$$

where $\tau_{c.m.}$ represents the center-of-mass neutrino lifetime. Taking into account the solar neutrino energy spectrum $\phi_\nu(E_\nu)$ one can write the expected gamma spectrum in the detector as:

$$\frac{dN}{dE_\gamma}(E_\gamma) = \frac{VT}{c}\int_{E_\gamma}^{E_{\nu\max}} \frac{dN}{dE_\gamma}(E_\gamma, E_\nu)\phi_\nu(E_\nu)dE_\nu, \quad (7)$$

where V is detector volume, T is time of measurement and c is the light speed in vacuum.

In the calculations we have used the neutrino fluxes given by the standard solar model (SSM)[30] and the neutrino energy spectra from [31]. The signal shapes (7) were convolved with the detector response function:

$$S(Q) = \int \frac{dN}{dT_e}(T_e(Q'))\frac{dT_e}{dQ}\mathrm{Res}(Q, Q')dQ' \qquad (8)$$

where $\mathrm{Res}(Q, Q')$ is the detector response function, σ_Q is defined by (2).

The Monte-Carlo method has been used in order to simulate the CTF response to gammas. The events were generated according to the spectrum given by (7) inside the inner vessel and in the adjacent water layer of 50 cm. The gamma-electron showers were followed using the EGS-4 code [32]. As soon as an electron of energy E_e appears inside the scintillator, the corresponding charge is added to the running sum, taking into account the quenching factor and the dependence of the registered charge on the distance from the detector's center. The obtained results for different α values are shown in fig.2.

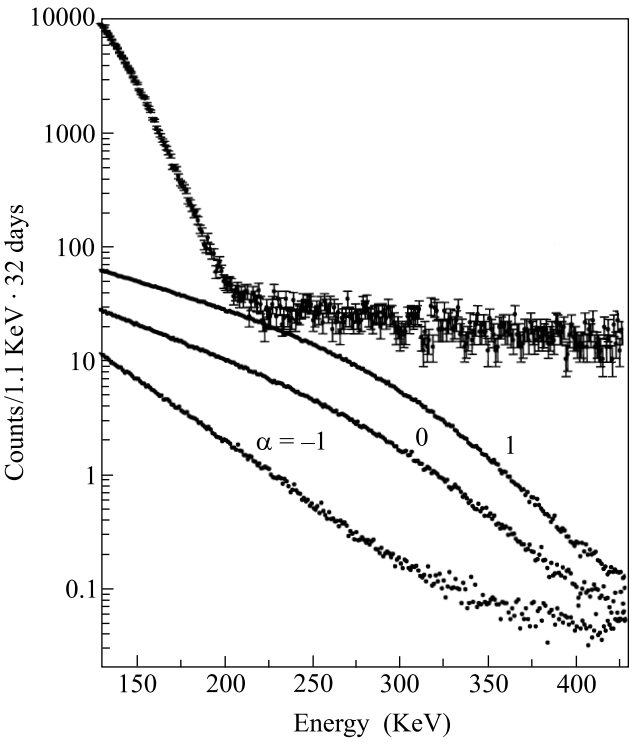

Fig.2. The experimental spectrum measured by CTF-II (upper plot with error bars) and the expected energy spectra from gammas appearing in radiative decay of the neutrino $\nu_H \to \nu_L + \gamma$ calculated by the M-C method with $\tau_{c.m.}/m_\nu = 5.0 \cdot 10^3$ s $\cdot$ eV^{-1} for 3 values of the parameter

Taking into account the best ratio of the expected effect to background, and in order to avoid systematic errors, caused by the uncertainty of the linear part of the

background at lower energies, the range 185–380 KeV has been chosen for the analysis. The maximum likelihood method was used to find the possible contribution from the radiative decay of the SSM solar neutrino in the measured spectrum. The likelihood function was found with the assumption that the number of counts in each channel of the measured spectrum $S_i^{\exp}$ obeys a normal distribution, and represents the sum of the model function describing the residual background (3) and the spectrum due to the neutrino decay calculated using (6)–(8).

The A, k_B and α parameters were fixed in the analysis at the values found during the data fitting in the wider region 138–380 KeV with much high statistics. The other three parameters were free. The changes in α and k_B do practically not influence the results of the analysis. The parameter A was also estimated independently from the measurements with a radon source.

The analysis of the upper limit on the life-time of the neutrino was performed in the following way. First, we minimized the $\chi^2(N_0, a, b, \tau_{c.m.}/m_\nu)$ value for different values of $\tau_{c.m.}/m_\nu$. The integration of the probability function gives a value of 0.9 (90% c.l.) for $\tau_{c.m.}/m_\nu = 4.2 \cdot 10^3$ s $\cdot$ eV^{-1} ($\alpha = 0$). This limit is practically independent of the lower bound of the analyzed region. The results of the optimal fit for value $\tau_{c.m.}/m_\nu = 4.2 \cdot 10^3$ s $\cdot$ eV^{-1} ($\alpha = 0$) are shown in fig.3. In the same way the upper limits $\tau_{c.m.}/m_\nu \geq 1.5 \cdot 10^3$ s $\cdot$ eV^{-1}($\alpha = -1$) and $\tau_{c.m.}/m_\nu \geq 9.7 \cdot 10^3$ s $\cdot$ eV^{-1}($\alpha = 1$) were obtained. Actually, the analysis of the CTF-II gives a 25% limit on the part of the background in the region 200–250 KeV attributed to the possible neutrino decay. The low sensitivity is explained by the similar behaviour of the background and the effect (small negative slope linear function). In principle, correct modeling of the ^{40}K background can eliminate the major part of the background that can finally lead to better results. The obtained values are more than one order of magnitude stronger than those obtained for low-energy neutrinos in direct experiments.

4. Using the data obtained with the prototype of the Borexino detector, the lower limit on the mean lifetime of pp- and ^{7}Be-neutrino relative radiative decay is obtained: $\tau_{c.m.}(\nu_H \to \nu_L + \gamma)/m_\nu \geq 4.2 \cdot 10^3$ s $\cdot$ eV^{-1} ($\alpha = 0$). It is more than one order of magnitude stronger than that obtained in previous experiments using nuclear reactors and accelerators. The CTF data can be used in the search for $\nu_H \to \nu_L + e^+ + e^-$ decays as well.

This job was performed with a support of the INFN Milano section in accordance to the scientific agreement on Borexino between INFN and JINR (Dubna). We would like especially to thank Prof. G. Bellini and Dr. G. Ranucci who organized our stay at the LNGS laboratory. Thanks to all our colleagues from the Borexino collaboration. We are very grateful to Richard Ford for the careful reading of the manuscript.

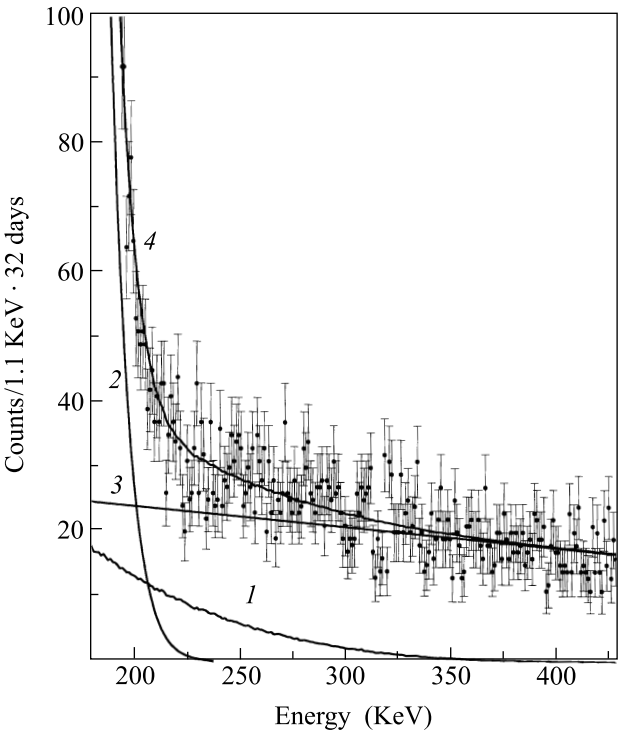

Fig.3. The fit in the region 185–380 KeV for the radiative neutrino decay: *1* – M-C calculation of the gamma spectrum from $\nu_H \to \nu_L + \gamma$ decay with $\tau_{c.m.}/m_\nu = 4.2 \cdot 10^3$ s $\cdot$ eV^{-1} ($\alpha = 0$); *2* – ^{14}C β-spectrum; *3* – linear background; *4* – total fit

1. B. W. Lee and R. E. Shrock, Phys. Rev. **D16** 1444 (1977).
2. S. T. Petcov, Yad. Fiz. **25**, 641 (1977).
3. E. Sato and M. Kobayashi, Prog. Theor. Phys. **58**, 1775 (1977).
4. M. A. Beg, W. J. Marciano, and M. Ruderman, Phys. Rev. **D17**, 1395 (1978).
5. A. De Rujula and S. L. Glashow, Phys. Rev. Lett. **45**, 942 (1980).
6. W. J. Marciano and A. Sirlin, Phys. Rev. **D22**, 2695 (1980).
7. P. B. Pal and L. Wolfenstein, Phys. Rev. **D25**, 766 (1982).
8. R. E. Shrock, Nucl. Phys. **B296**, 359 (1982).
9. F. Boem and P. Vogel, *Physics of massive neutrinos*, Cambridge University Press, 1992.
10. F. Reines et al., Phys. Rev. Lett. **32**, 180 (1974).
11. P. Vogel, Phys. Rev. **D30**, 1505 (1984).
12. G. Zacek et al., Phys. Rev. **D34**, 2621 (1986).

13. L. Oberauer, F. Von Feilitzsch, and R. L. Mossbauer, Phys. Lett. **B198**, 113 (1987).
14. A. V. Derbin et al., JETP Lett. **57**, 768 (1993).
15. D. A. Krakauer et al., Phys. Rev. **D44**, 44 (1991).
16. G. G. Raffelt, Phys. Rev. **D31**, 3002 (1985).
17. D. E. Groom et al. (Particle Data Group), Eur. Phys. Jour. **C15**, 1 (2000).
18. L. Oberauer et al., Astrpart. Phys. **1**, 377 (1993).
19. G. G. Raffelt, Phys. Rep. **320**, 319 (1999).
20. G. Alimonti et al., Borexino coll., Astroparticle Phys. **18**, 1 (2002).
21. G. Ranucci et al., Nucl. Instr. Meth. **A333**, 553 (1993).
22. G. Alimonti et al., Borexino coll., Nucl. Instr. Meth. **A406**, 411 (1998).
23. G. Alimonti et al., Borexino coll., Phys. Lett. **B422**, 349 (1998).
24. G. Alimonti et al., Borexino coll., Astroparticle Phys. **8**, 141 (1998).
25. G. Alimonti et al., Borexino coll., Nucl. Instr. Meth. **A440**, 360 (2000).
26. J. B. Birks, Proc. Phys. Soc. **A64**, 874 (1951).
27. H. O. Back et al., Borexino coll., Phys. Lett. **B525**, 29 (2002).
28. O. Ju. Smirnov, LNGS preprint INFN TC/00/17, accepted by PTE(2002).
29. V. V. Kuzminov and N. Ja. Osetrova, Phys. At. Nucl. **63**, 1292 (2000).
30. J. N. Bahcall, H. Pinsonneault, and S. Basu, Astrophys. J. **555**, 990 (2001).
31. J. N. Bahcall, Phys. Rev. **C56**, 3391 (1997).
32. W. R. Nelson, H. Hirayama, and D. W. O. Rogers, The EGS4 code system, SLAC-265, 1985.